Mesh-Free Collocation Based for Phase Transformations in Alloys

Sayed A. Zaki [1], Taher A. Nofal [2] S. G. Ahmed [3]

[1] *Assistant Professor of Mathematics,* [2] *Associate Professor of Mathematics,* [3] *Professor of Engineering Mathematics and Numerical Analysis Department of Mathematics, College of Science, Taif University, Taif-Al-Haweiah, Kingdom of Saudi Arabia*

***Abstract*-In the present paper, a new applied algorithm based a new composite radial basis designed to solve binary alloy problem. The collocation mesh-free based the suggested radial basis function is used as a mathematical tool for the solution procedure. The advantage of such new radial basis function is that it can overcome the singularity in the diagonal matrix of the stiffness matrix resulted due to collocation procedure. The inverse matrix inversion is also used to solve two systems of linear equations at any two successive time steps. Two different examples are solved and some of the computed results are compared with the available analytical results. The computed results gave a promise to solve higher dimensional problems and can be extended to cover ternary alloys.**

***Keywords-Moving boundary problems, Phase transformation, Binary alloys, Radial basis functions, Collocation techniques*.**

I. INTRODUCTION

Heat treatment of metals is often necessary to optimize their mechanical properties both for further processing and final use during the heat treatment the metallurgical state of the alloy changes **[1-2]**. This change can either involve the phases being present or the morphology of the various phases **[3]**. Aluminum alloys usually contain precipitates and in-homogeneities, these in-homogeneities can be removed with a thermal treatment, during which the precipitates dissolve. Although precipitate dissolution is not the only metallurgical process-taking place during homogenization, it is often the most critical of the processes occurring. Precipitates dissolution can be modeled as one, two or three moving boundary problem. Till now, there are neither general models for micro structural changes nor general models for the kinetics of these changes **[4-5]**. Models describing the process as a moving boundary problem is also, referred to as Stefan problems **[6]**. In recent years, the simpler models covering binary and ternary alloys have been extended to cover multi-component particles **[7]**. Due to the complex nature of the moving boundary problems very few analytical solutions are available and limited to infinite or semi-infinite domain problems. Existence and uniqueness of analytical solutions had been proved by Evan and Douglas, respectively in **[8-9]**. For long time researchers recognized problems such as, labor intensive, time-consuming and error-prone task when using a mesh-based method such as finite element method **[10]**. One way for their efforts to overcome these problems was the automatic mesh generation, the second way to overcome such problems was developing the mesh-less methods. Mesh-less methods for solving boundary value problems have been extensively popularized owing to their flexibility in engineering applications, especially for problems with discontinuities and because of high accuracy of the computed results **[11]**. Mesh-free methods do not require a mesh to discretize the domain of the problem under consideration, and the approximate solution is constructed entirely based on a set of scattered nodes.

II. MATHEMATICAL FORMULATION

Consider a domain $\Omega = [0, \ell]$ that is composed by a particle whose domain is denoted by $\Omega_{part} = [0, s(t))$ and diffusive phase $\Omega_{dif\ ph} = (s(t), \ell]$. We consider the concentration $c(x,t)$ of certain material within $\Omega = \Omega_{part} \cup \Omega_{dif\ ph}$. Assume the concentration of the particle is constant and denoted by c_{part}. The configuration of the problem is shown in figure (1).

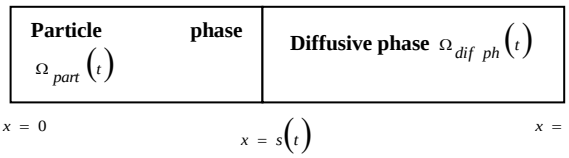

Figure 1: Problem configuration

The state equations with the associated boundary and initial conditions are as follow:

$$c(x,t) = c_{part} \qquad x \in \Omega_{part} = [0, s(t)), \quad t > 0$$

(1)

$$\frac{\partial c(x,t)}{\partial t} = \frac{\partial}{\partial x}\left(D \frac{\partial c(x,t)}{\partial x} \right), x \in \Omega_{dif\ ph} = (s(t), \ell], \quad t > 0$$

(2)

It is assumed in the model that there is no concentration transport, *i.e.*,

$$\frac{\partial c(x,t)}{\partial x} = 0, x \in \partial\Omega,\ \partial\Omega = 0 \quad \text{or} \quad \ell,\ t \geq 0$$

(3)

Assume also a piecewise initial concentration of the form:

$$c(x,t) = \begin{cases} c_{part} & 0 \leq x < s_0 \\ c_{sol} & x = s_0 \\ c_0 & s_0 < x \leq \ell \end{cases} \quad (4)$$

Last condition represents the mass balance of atoms transferred to the diffusive phase:

$$\frac{ds(t)}{dt}\left(c_{part} - c(s(t),t) = c_{sol}\right) = D\frac{\partial c(x,t)}{\partial x}, x = s(t),\ t > 0 \quad (5)$$

III. THE PROPOSED METHOD

Consider a three-dimensional heat transfer problem defined as:

$$\frac{\partial c(\mathrm{x},t)}{\partial t} = k\nabla^2 c(\mathrm{x},t) \qquad \mathrm{x}, y, z \in \partial\Omega$$

(6)

With

$$\xi_1 c(\mathrm{x},t) + \xi_2 \nabla c'(\mathrm{x},t) = f(\mathrm{x},t) \qquad \mathrm{x} \in \partial\Omega$$

(7)

$$c(\mathrm{x},t) = c_0(t)$$

(8)

Starting with implicit $\Theta-$weighted scheme, therefore equation (6) will be:

$$\frac{c(\mathrm{x},t+\Delta t) - c(\mathrm{x},t)}{\Delta t} = k\left(\Theta\nabla^2 c(\mathrm{x},t+\Delta t) + (1-\Theta)\nabla^2 c(\mathrm{x},t)\right)$$

(9)

Re-arrange and simplify, leads to:

$$\left(1+\alpha\nabla^2\right)c^{n+1} = \left(1+\beta\nabla^2\right)c^n$$

(10)

Where

$$\alpha = -k\Theta(\Delta t) \quad (11)$$

$$\beta = k(1-\Theta)(\Delta t)$$

(12)

Assume that the potential can be approximated as follows:

$$u(\mathrm{x}) \cong \sum_{j=1}^{N} \lambda_j \left[\varepsilon\varphi_{1j}(r_{ij}) + (1-\varepsilon)\varphi_{2j}(r_{ij})\right]$$

(13)

In Equation (13) the radial basis function can be used in the computation as follows:

$$\varphi_{kj}(r_{ij}) = \begin{cases} \varphi_{1j}(r_{ij}) & \varepsilon = 1 \quad for \quad i = j, \quad k = 1 \\ \varphi_{2j}(r_{ij}) & \varepsilon = 0 \quad for \quad i \neq j, \quad k = 2 \end{cases}$$

(14)

In equation (13):

$$\varphi_{1j}(r_{ij}) = \text{Cubic} = r_{ij}^3$$

(15)

$$\varphi_{2j}(r_{ij}) = \text{TP} = r_{ij}^{2m}\log(r_{ij})$$

(16)

The linear operator ℓC can be approximated as follows:

$$\ell(c(\mathrm{x})) \cong \sum_{j=1}^{N} \ell\left\{\lambda_j\left[\varepsilon\varphi_1(r_{ij}) + (1-\varepsilon)\varphi_2(r_{ij})\right]\right\}$$

(17)

By making use the concept of equation (17), equation (10), takes the form:

$$\sum_{j=1}^{N} \lambda_j^{n+1}\left(1+\alpha\nabla^2\right)\left[\varepsilon\varphi_{1j}(r_{ij}) + (1-\varepsilon)\varphi_{2j}(r_{ij})\right]$$

$$= \sum_{j=1}^{N} \lambda_j^{n}\left(1+\beta\nabla^2\right)\left[\varepsilon\varphi_{1j}(r_{ij}) + (1-\varepsilon)\varphi_{2j}(r_{ij})\right]$$

(19)

Let for simplicity:

$$\Psi(r_{ij}) = \left[\varepsilon\varphi_{1j}(r_{ij}) + (1-\varepsilon)\varphi_{2j}(r_{ij})\right]$$

(20)

By making use of equation (20) into equation (19), the later will take the following simplified form:

$$\sum_{j=1}^{N} \lambda_j^{n+1}\left(1+\alpha\nabla^2\right)\Psi(r_{ij}) = \sum_{j=1}^{N} \lambda_j^{n}\left(1+\beta\nabla^2\right)\Psi(r_{ij})$$

(21)

By making use of equation (20) into equation (3), leads to:

$$\sum_{j=1}^{N} \lambda_j^{n}\left[3\varepsilon r_{ij}^2 + (1-\varepsilon)r_{ij}\left(1+2\log r_{ij}\right)\right] = 0$$

(22)

By making use of equation (20) into equation (5), leads to:

$$\frac{ds(t)}{dt}\left(c_{part} - c(s(t),t) = c_{sol}\right) =$$

$$D\sum_{j=1}^{N} \lambda_j^{n}\left[3\varepsilon r_{ij}^2 + (1-\varepsilon)r_{ij}\left(1+2\log r_{ij}\right)\right], x = s(t),\ t > 0$$

(23)

In equation (23), let us approximate the velocity of the moving boundary using forward approximation as follows:

$$\frac{ds(t)}{dt} = \frac{s^{n+1} - s^n}{\Delta t}$$

(24)

By making use of equation (24) into equation (23), then the later will take the following form:

$$s^{n+1} = s^n + \frac{D\Delta t}{\left(c_{part} - c_{sol}\right)}\sum_{j=1}^{N} \lambda_j^{n}\left[3\varepsilon r_{ij}^2 + (1-\varepsilon)r_{ij}\left(1+2\log r_{ij}\right)\right]$$

(25)

It is emphasized to take the simplification that will occur in both equations (22) and (25) when dealing with these equations. According to the suggested radial basis function, the control parameter automatically will be zero at the extreme points of the domain therefore equations (22) and (25) will take the following forms, respectively:

$$\sum_{j=1}^{N} \lambda_j^n \left[r_{ij} \left(1 + 2 \log r_{ij} \right) \right] = 0$$

(26)

$$s^{n+1} = s^n + \frac{D\Delta t}{\left(c_{part} - c_{sol} \right)} \sum_{j=1}^{N} \lambda_j^n \left[r_{ij} \left(1 + 2 \log r_{ij} \right) \right]$$

(27)

IV. SOLUTION PROCEDURE

Let us start dealing with equation (21) and taking the following simplifications into consideration, as follows:

$$\Psi_1 \left(r_{ij} \right) = \left(1 + \alpha \nabla^2 \right) \Psi \left(r_{ij} \right)$$

$$\Psi_2 \left(r_{ij} \right) = \left(1 + \beta \nabla^2 \right) \Psi \left(r_{ij} \right)$$

(28)

Now then, equation (21) with the help of equation (28), will take the following new form:

$$\sum_{j=1}^{N} \lambda_j^{n+1} \Psi_1 \left(r_{ij} \right) = \sum_{j=1}^{N} \lambda_j^n \Psi_2 \left(r_{ij} \right)$$

(29)

Equation (29) in a matrix form will be:

$$\begin{bmatrix} \Psi_1(r_{21}) & \Psi_1(r_{12}) \ldots\ldots \Psi_1(r_{1,N}) \\ \Psi_1(r_{21}) & \Psi_1(r_{22}) \ldots\ldots \Psi_1(r_{2,N}) \\ \Psi_1(r_{31}) & \Psi_1(r_{32}) \ldots\ldots \Psi_1(r_{3,N}) \\ \ldots\ldots\ldots\ldots\ldots\ldots \\ \ldots\ldots\ldots\ldots\ldots\ldots \\ \Psi_1(r_{N,1}) & \Psi_1(r_{N,2}) \ldots \Psi_1(r_{N,N}) \end{bmatrix} \begin{bmatrix} \lambda_1 \\ \lambda_2 \\ \lambda_3 \\ \ldots\ldots \\ \ldots\ldots \\ \lambda_{11} \end{bmatrix}^{n+1}$$

$$= \begin{bmatrix} \Psi_2(r_{21}) & \Psi_2(r_{12}) \ldots\ldots \Psi_2(r_{1,N}) \\ \Psi_2(r_{21}) & \Psi_2(r_{22}) \ldots\ldots \Psi_2(r_{2,N}) \\ \Psi_2(r_{31}) & \Psi_2(r_{32}) \ldots\ldots \Psi_2(r_{3,N}) \\ \ldots\ldots\ldots\ldots\ldots\ldots \\ \ldots\ldots\ldots\ldots\ldots\ldots \\ \Psi_2(r_{N,1}) & \Psi_2(r_{N,2}) \ldots \Psi_2(r_{N,N}) \end{bmatrix} \begin{bmatrix} \lambda_1 \\ \lambda_2 \\ \lambda_3 \\ \ldots\ldots \\ \ldots\ldots \\ \lambda_{11} \end{bmatrix}^{n}$$

(30)

Equation (30) is the key note of starting solution procedure, i.e., at the starting time, we will start solution by dealing with the right hand side of it, this can be done as follows:

$$\begin{bmatrix} \Psi_2(r_{21}) & \Psi_2(r_{12}) \ldots\ldots \Psi_2(r_{1,N}) \\ \Psi_2(r_{21}) & \Psi_2(r_{22}) \ldots\ldots \Psi_2(r_{2,N}) \\ \Psi_2(r_{31}) & \Psi_2(r_{32}) \ldots\ldots \Psi_2(r_{3,N}) \\ \ldots\ldots\ldots\ldots\ldots\ldots \\ \ldots\ldots\ldots\ldots\ldots\ldots \\ \Psi_2(r_{N,1}) & \Psi_2(r_{N,2}) \ldots \Psi_2(r_{N,N}) \end{bmatrix} \begin{bmatrix} \lambda_1 \\ \lambda_2 \\ \lambda_3 \\ \ldots\ldots \\ \ldots\ldots \\ \lambda_{11} \end{bmatrix}^{n} = \begin{bmatrix} c(x_1) \\ c(x_2) \\ c(x_3) \\ \ldots\ldots \\ \ldots\ldots \\ c(x_N) \end{bmatrix}$$

(31)

The system given by equation (31) in a compact form:

$$\Psi_2 \left(r_{ij} \right) \lambda^n = C(x)$$

(32)

The solution of the system given by equation (32) using matrix inversion method will be as follows:

$$\lambda^n = \Psi_2^{-1} \left(r_{ij} \right) C(x)$$

(33)

The successive time steps solutions come from the fact that the right hand side of the system (30) becomes known at the time level n. Now equate the left hand side of the same system by known vector B, then the system takes the following new form:

$$\Psi_1 \left(r_{ij} \right) \lambda^{n+1} = B$$

(34)

Again using matrix inversion method, we can get the solution of the system given by equation (34):

$$\lambda^{n+1} = \Psi_1^{-1} \left(r_{ij} \right) B$$

(35)

Now we can summarize the computation procedure in the following flow chart shown in figure (2).

V. NUMERICAL RESULTS

Two different test problems are solved, the numerical data for both are given in the following table (1) **[12]**:

Test problem (1)

The movement of the moving boundary is compared with the similarity solution as shown in figure (3), as it is appear the present solution is very close to the analytical similarity solution. In the beginning of the time and up to time nearly equal 0.3 an agreement between the two solutions with some errors can be neglected, after that the error increases but still within the acceptable behavior.

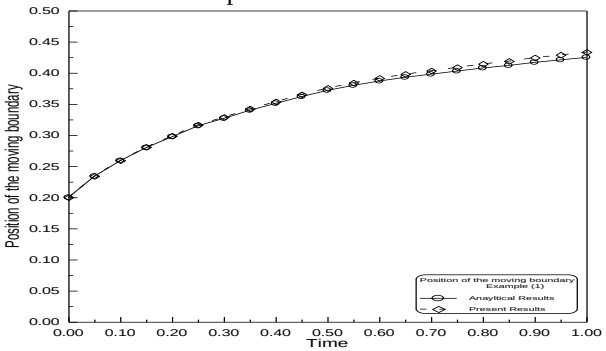

Figure 3: Location of the moving boundary-Example (1)

The concentration is computed at three different times, 0.01, 0.03, and 0.05 against space variable *x*, as shown in figures (4-6) and compared with previous numerical results. As it is clear the concentration in the particle domain is always constant and equals to the boundary condition 0.53. On the other side the concentration in the diffusive phase starts at the point very close to the moving boundary at the time of computations. Therefore, the starting point of these three

curves is different from case to another due to the position of the moving boundary at these times.

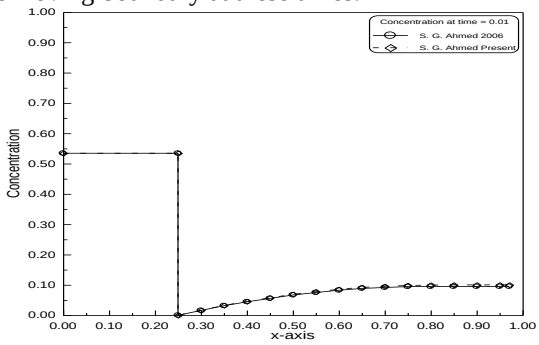

Figure 4: Concentration at time 0.01

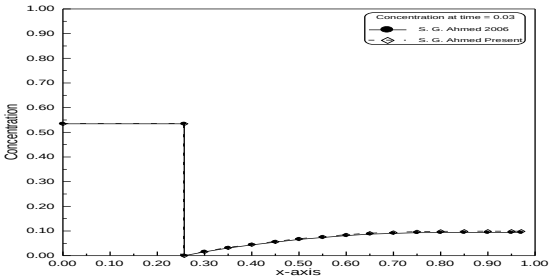

Figure (5): Concentration at time 0.03

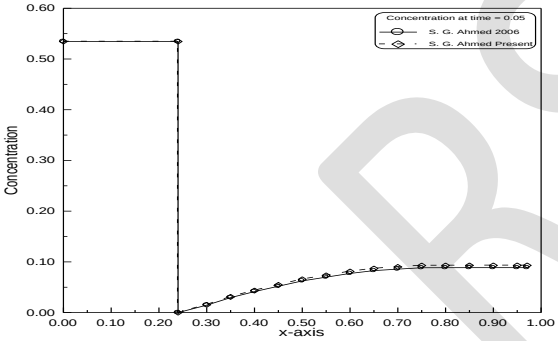

Figure (6): Concentration at time 0.05

The behavior of the concentration versus time at three different points inside the domain, 0.25, 0.35, and 0.45 is also computed and the results are shown in figures (7-9), respectively.

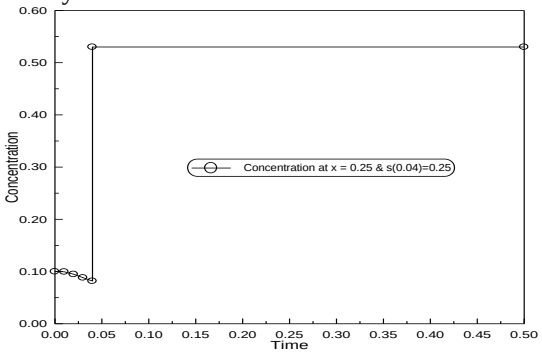

Figure (7): Concentration at x = 0.25

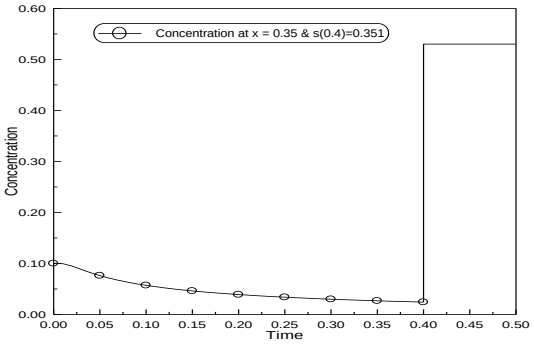

Figure (8): Concentration at x = 0.35

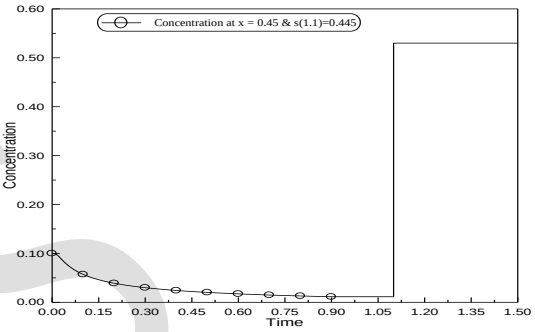

Figure (9): Concentration at x = 0.45

It is clear from figures (7-9) that the concentrations at time zero equal the initial condition. The behavior of the concentration after that decreases till the concentration at the moving boundary, then jump in the concentration profile occur at behave constant value at equal to the particle concentration.

Test problem (2)

For the second test problem, the moving boundary is plotted in figure (10) resulting from the present solution and the corresponding analytical solution. It can be seen that the error between the two solutions is small and can be neglected. As time proceeds the present solution starts to deviate but the error still small.

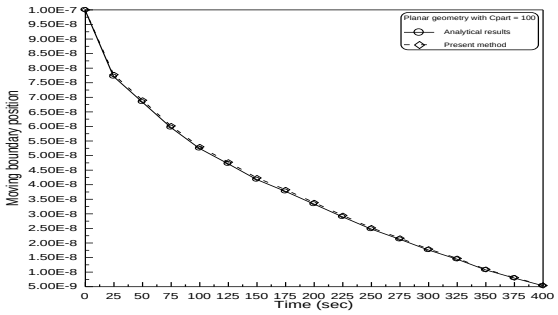

Figure (10): Moving Boundary for test problem (2)

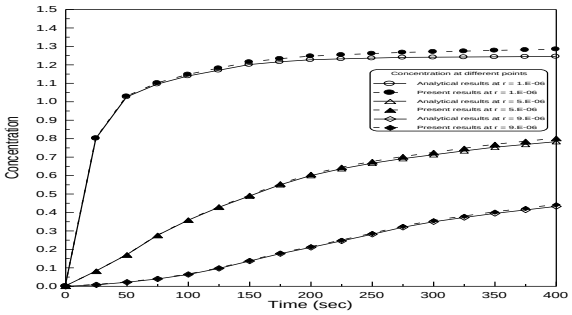

Figure (11): Variation of concentration for test problem (2)

It can be seen from figure (11) that, the concentration at the three points has an exponentially increasing. Also at the same time the concentration at the point near the outer surface is small compared with the concentration at the point far away from it and this also agrees with the physics of the problem.

CONCLUSION

Due to the lack of mesh-less methods for solving alloys problems, we focus our attention to try solving these type of problems. One of these methods is the collocation, but usually we encounter singularity problem especially when using thin plate radial basis function. Due to this difficulty we suggested a composite radial basis function consists of superposition of both cubic and thin plate radial basis functions connected by a control parameter which take only single value zero or one. When dealing with diagonal elements we will use the cubic radial basis function and for the rest of the stiffness matrix elements we will use the thin plate radial basis function due to its high accuracy. A generalized algorithm is also designated to cover high dimensional problems as well as ternary and multi-component alloys. The accuracy of the results due to the suggested radial basis function and the proposed generalized algorithm is acceptable and promise more improvement in the future works.

REFERENCES

[1] Chen, S., Merriman, B., Osher, S. and Smereka, P.,' A simple level set method for solving Stefan problems', J. Comput. Phys., Vol. 135, pp. 8-29, 1997.

[2] Ahmed S.G.,' A numerical method for oxygen diffusion and absorption in a sike cell', Applied Mathematics and Computations, Netherlands, In press, available on line on www.sciencedirect.com, 2005.

[3] Juric, D. and Tryggvason, G.,' A front tracking method for dendritic solidification', J. Comput. Phys., Vol. 123, pp. 127-148, 1996.

[4] Vuik, C. and Cuvelier, C.,' Numerical solution of an etching problem', J. Comput. Phys., Vol. 59, pp. 247-263, 1985.

[5] Ahmed, S. G., 'A semi-analytical method for phase change transformation in binary alloys', Journal of Computational and Applied Mathematics, Netherlands, Available online, August, 2006

[6] Javierre, E. et. al.,' A comparison of numerical methods for one-dimensional Stefan problems', In press, Available on line at www.sciencedirect.com, 2005.

[7] Vermolen, F., Vuik, C. and Zwaag, S.,' A mathematical model for the dissolution of stoichiometric particles in multi-component alloys' Materials Science and Engineering, A328, pp. 14-25, 2002.

[8] Evans, G.W.,' A note on the existence of a solution to a problem of Stefan', Q. Appl. Math., Vol. 9, pp. 185-193, 1951.

[9] Douglas, J.,' A uniqueness theorem for the solution of a Stefan problem', Proc. Annu. Math. Soc. 8, pp. 402-408, 1957.

[10] Lee, J.K. and Froechlich, D.C.,' Review of literature on the finite-element solution of the equation of two-dimensional surface water flows in the horizontal plane', US Geological Survey Circular 1009, 1986.

[11] Zhu, T., Zhang, J. and Atluri, S.N.,' A meshless numerical method based on the local boundary integral equation (LBIE) to solve linear and non-linear boundary value problems', Engineering Analysis with Boundary Elements, Vol. 23, pp. 375-389, 1999.

[12] S. G. Ahmed, 'A semi-analytical method for phase change transformation in binary alloys', Journal of Computational and Applied Mathematics, Netherlands, Available online, August, 2006.

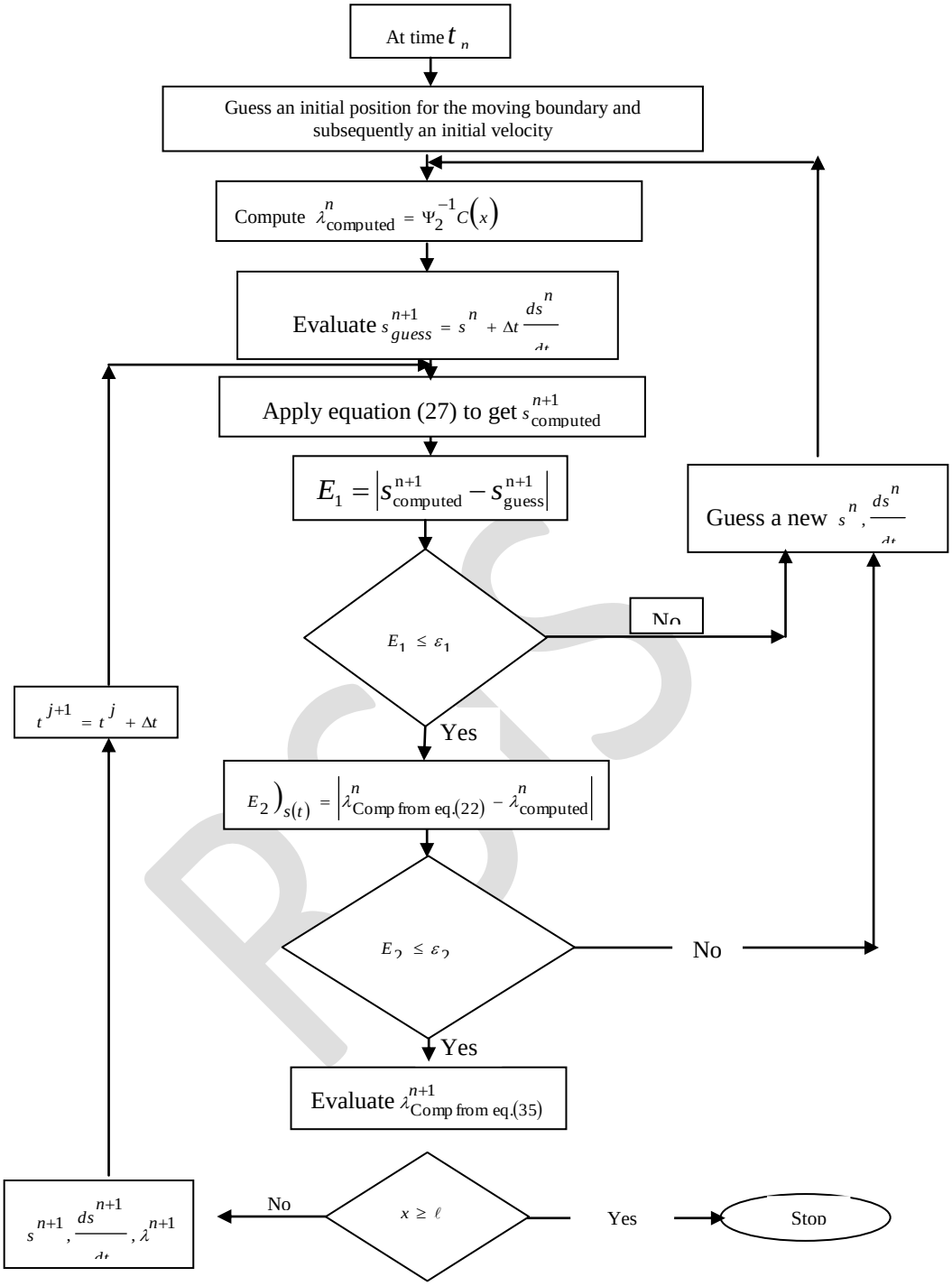

Figure (2)

Table 1: Numerical data

	C_{Part}	C_o	ℓ	s_0	D
Test problem (1)	0.53	0.1	1.0	0.2	1
Test problem (2)	100	0	$0.1\times10^{-4}\,m$	$0.1\times10^{-6}\,m$	$10^{-13} m^2/\text{sec}$